Microwave Conductance of Semicontinuous Metallic Films from Coplanar Waveguide Scattering Parameters

J. Obrzut and O. Kirillov

National Institute of Standards and Technology
Gaithersburg, MD 20899, U.S.A.
jan.obrzut@nist.gov, oleg.kirillov@nist.gov

***Abstract*—Conductance of thin semicontinuous metallic films is measured in coplanar waveguide configuration at frequencies of 1 GHz to 20 GHz. The presented model of the microwave network correlates the experimental scattering parameters (S_{11}) and (S_{21}) with complex impedance and propagation constant, from which we are able to determine the films surface conductance, coefficients of reflectance, transmittance and dissipation. The measurement is illustrated on films of gold, 4 nm to 12 nm thick. After percolation from individual nanoparticles, films thicker than 10 nm resemble a continuous conductor. The presented methodology accurately captures the insulator to conductor transition, and can be used to determine microwave characteristics of such materials**.

Keywords— coplanar waveguides; microwave conductivity; thin metallic films; conductivity percolation.

I. INTRODUCTION

Metallic films deposited from vapor typically consist of a semicontinuous random structure, which evolves from an electrically insulating into a conducting percolated network [1]. This transition can be accurately captured by the microwave transition-reflection measurements. Near percolation the film material simultaneously exhibits dielectric and conducting characteristics, and both of these contribute to transmitted, reflected and absorbed waves in specific ways. In the microwave range, the conductivity of thin metallic films is typically measured by one-port microwave reflectometry [2]. In this configuration, however, only the reflected wave is measured, and thus the transmitted and absorbed waves cannot be accurately determined.

In this paper we present microwave measurements of the ac conductance of thin metallic films from transmitted and reflected waves in a coplanar waveguide configuration [3, 4]. The presented model of the microwave network correlates the experimental scattering parameters, (S_{11}) and (S_{21}), with complex impedance and propagation constant from which we determine the film surface conductance. We illustrate the measurement results using vapor deposited gold as representative of semi-continuous thin film conductors, which during deposition undergo an insulator to conductor transition. Our results can be extended to characterize other nano-structured thin film materials which are increasingly being investigated for modern electronics and other emerging technologies.

II. EXPERIMENTAL PROCEURES AND METHODS

Coplanar waveguides (CPW) with a nominal characteristic impedance value (Z_0) of 50 Ω and a propagation length (l) ranging from 450 µm to 1800 µm were made with 10 nm Ti and 200 nm gold evaporated onto 500 µm thick, 25 mm by 25 mm electronic-grade alumina substrates. CPWs were patterned by liftoff lithography. The width (w) of the central signal strip of these CPWs was 50 µm ± 0.2 µm, while the signal to ground plane spacing (s) was nominally 22 µm (Fig. 1). In order to compensate for manufacturing tolerances, the CPWs were arranged in several groups, each with ground plane spacing differing from the nominal value in steps of 1 µm, which covers Z_0 values from 49 Ω to 51 Ω. We selected CPWs

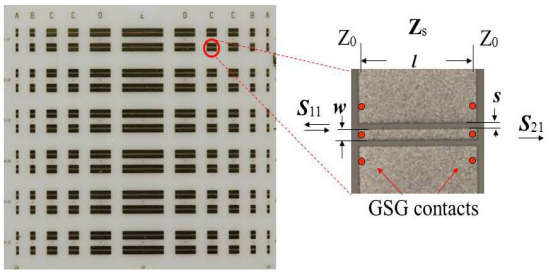

Figure 1. Wafer test structure (left) and corresponding dimensions (right) of a coplanar waveguide.

having Z_0 between 49.5 Ω to 50.5 Ω for the experiment.

Thin films of gold (Au) were deposited by the thermal evaporation of gold directly onto CPWs through a shadow mask, leaving reference CPWs uncoated.

Measurements of the S_{11} and S_{21} parameters were performed using an HP 8720D network analyzer connected to the CPW test structure with phase preserving cables from Agilent (85131-60013) and co-planar GSG air-coplanar probes (ACP-40, 100 µm pitch) from Cascade. The system was calibrated using a thru-reflection-match (TRM) calibration

Official contribution of the National Institute of Standards and Technology, not subject to copyright in the United States.

procedure using WinCal calibration software and a 101-190C impedance calibration standard from Cascade. The impedance characteristic of the uncoated CPWs was used as a reference.

The combined uncertainty of scattering parameters magnitude is 5×10^{-4} and phase angle is 0.1 Rd.

Microwave Network Model of CPW Test Structure

We consider the CPW test structure as a microwave network consisting of impedance discontinuity Z_0;$\boldsymbol{Z}_s$;Z_0. Thereby, $\boldsymbol{Z}_s$ is inserted between two reference transmission lines having a real characteristic impedance Z_0 (figure 1). Multiple wave reflections that take place at each Z_0;$\boldsymbol{Z}_s$ interface are accounted by the model [5]. The electrical characteristic of the film in the specimen section is represented by a complex impedance $\boldsymbol{Z}_s$, and the corresponding equivalent circuit of linearly distributed shunt capacitance (C_s), conductance (G_s), series inductance (L_s) and resistance (R_s) [6]. If the length (l) of the specimen was infinite, then the reflection coefficient $\boldsymbol{\Gamma}$ of a wave incident on the interface from the CPW would be given simply by $\boldsymbol{S}_{11}$. In the case of a finite propagation length, l, the amplitudes of the transmitted and reflected waves depend also on the transmission coefficient $e^{-\gamma l}$, where $\boldsymbol{\gamma}$ is the complex propagation constant. The solution of the network for the scattering parameters $\boldsymbol{S}_{11}$ and $\boldsymbol{S}_{21}$ are given by (1) and (2) respectively [7]:

$$\boldsymbol{S}_{11} = \frac{\boldsymbol{\Gamma}(1-e^{-\gamma l})(1+e^{-\gamma l})}{1-\boldsymbol{\Gamma}^2 e^{-2\gamma l}} \qquad (1a)$$

$$\boldsymbol{S}_{21} = \frac{e^{-\gamma l}(1-\boldsymbol{\Gamma})(1+\boldsymbol{\Gamma})}{1-\boldsymbol{\Gamma}^2 e^{-2\gamma l}} \qquad (1b)$$

where, $\boldsymbol{S}_{11}$ and $\boldsymbol{S}_{21}$ are the measured complex scattering parameters, $\boldsymbol{\gamma}=\alpha+j\beta$ is the complex propagation constant, l is the propagation length, and $\boldsymbol{\Gamma}$ is the complex reflection coefficient [6, 8].

$$\boldsymbol{Z}_s = Z_0(1+\boldsymbol{\Gamma})/(1-\boldsymbol{\Gamma}) \qquad (2)$$

It can be shown that solution of the network equations (1) for $\boldsymbol{Z}_s$ and $\boldsymbol{\gamma}$ is given by (3) [10]:

$$e^{-\gamma l} = \left[\frac{1-\boldsymbol{S}_{11}^2+\boldsymbol{S}_{21}^2)}{2\boldsymbol{S}_{11}} \pm \sqrt{\boldsymbol{K}}\right]^{-1} \qquad (3a)$$

$$\boldsymbol{K} = \frac{(\boldsymbol{S}_{11}^2+\boldsymbol{S}_{21}^2+1)^2-(2\boldsymbol{S}_{11})^2}{(2\boldsymbol{S}_{11})^2} \qquad (3b)$$

$$\boldsymbol{Z}_s = Z_0\left[\frac{(1+\boldsymbol{S}_{11})^2-(\boldsymbol{S}_{21})^2}{(1-\boldsymbol{S}_{11})^2-\boldsymbol{S}_{21})^2}\right]^{\frac{1}{2}} \qquad (3c)$$

Once $\boldsymbol{\gamma}$ and $\boldsymbol{Z}_s$ are obtained, the distributed conductance G_s, can be determined by the conventional transmission line relations [6, 9]:

$$G_s = \mathrm{Re}(\boldsymbol{\gamma}/\boldsymbol{Z}_s) \qquad (4)$$

In order to determine the values of $\boldsymbol{\gamma}_s$ and $\boldsymbol{Z}_s$ from (3), the measured complex $\boldsymbol{S}_{11}$ and $\boldsymbol{S}_{21}$ parameters should be returned by the network analyzer in the form complex coordinates i.e., $\boldsymbol{S}_{ij}$= (Re$\boldsymbol{S}_{ij}$, Im$\boldsymbol{S}_{ij}$). The phase angle needs to be converted to the true value of the measured phase φ in radians, rather than the cyclically mapped phase angle ±180°. Results with no physical meaning such as a negative attenuation constant (α) need to be corrected by selecting an appropriate solution from (3). For longer CPWs, for which the phase angle of $\boldsymbol{S}_{21}$ is larger than π, the selection of a physically relevant solution of (3a-c) is not intuitive and often becomes numerically involved. The distributed conductance (G_s), Eq. 4, can be correlated with the film surface conductance (σ_s), $\sigma_s = G_s \cdot s/2$ (in units of Siemens per square), where (s) is the CPW signal to ground plane spacing. Here, $s = 22 \times 10^{-4}$ cm (figure 1). By normalizing σ_s to the thickness (d) of the film, G_s can be scaled further to obtain the material's volume conductivity, $\sigma_v = \sigma_s / d$.

III. Resulst and Discussion

A. Scattering Parameters

Figure 2 shows example measurements of the magnitude and phase of the complex scattering parameters $\boldsymbol{S}_{21}$ measured for 900 μm long uncoated CPWs (plots 1) and for CPWs coated with gold films with thickness increasing from 4 nm to 10 nm (plots 2-7). The uncoated reference CPWs have a highly transmitting characteristic with the relative magnitude of the transmitted wave, $|\boldsymbol{S}_{21}|$, slightly decreasing with frequency from its maximum value of 1.0 (Fig. 2a plot 1). In comparison, the relative magnitude of the reflected wave, $|\boldsymbol{S}_{11}|$, (not shown) is rather small, in the range 3×10^{-3} (–50 dB). This indicates that that the impedance miss-matching of the uncoated CPWs is not significant. The $\boldsymbol{S}_{21}$ phase angle, φ, shown in Fig. 2b changes linearly with frequency, with constant phase velocity β. At any given frequency, the phase angle can be expressed as proportional to the electrical length, $\varphi = \beta l_E$. Fig. 2b shows that with increasing film thickness, electrical length l_E becomes longer, or equivalently, the propagation velocity decreases and the guided wave λ_g becomes more compressed. The constant, frequency independent value of β and compression of the guided wave ($\lambda_g < \lambda_0$) are characteristic of the TEM propagation mode. These observations confirm the applicability of the quasi - TEM model to our experiment [7]. We observe a general tendency of conducting Au films to affect the magnitude and phase of both the $\boldsymbol{S}_{11}$ and $\boldsymbol{S}_{21}$ parameters. With increasing film thickness, the magnitude of $\boldsymbol{S}_{11}$ increases, while the magnitude of $\boldsymbol{S}_{21}$ correspondingly

Certain commercial equipment, instruments, or materials are identified in this paper in order to specify the experimental procedure adequately.
Such identification is not intended to imply recommendation or endorsement by the National Institute of Standards and Technology, nor is it intended to imply that the materials or equipment identified are necessarily the best available for the purpose

decreases. These changes captured by our measurements are significant, and reflect the increasingly conducting character of the films. As the film thickness grows, $|\boldsymbol{S}_{11}|$ increases towards the maximum of 1.0 (0 dB) while the phase angle approaches the value of π. An abrupt change in $\boldsymbol{S}_{11}$ phase, from about $-\pi$ to $+\pi$ is observed when the film thickness increases from 7 nm to 8 nm, indicating a transition from an insulator to a conductor. Films thicker than 7 nm are clearly conducting, each showing $|\boldsymbol{S}_{11}|$ values approaching 1.0 and phase angles of about π. In contrast to $\boldsymbol{S}_{11}$, the magnitude and phase of $\boldsymbol{S}_{21}$ (figure 2) evolves with film thickness more gradually showing a higher sensitivity to these thicker, more conducting films. Thus, in comparison to the simple one-port $\boldsymbol{S}_{11}$ reflectometry, measurement of both, $\boldsymbol{S}_{11}$ and $\boldsymbol{S}_{21}$ enable the accurate capture and measurement of the transition from the insulating to the conducting state.

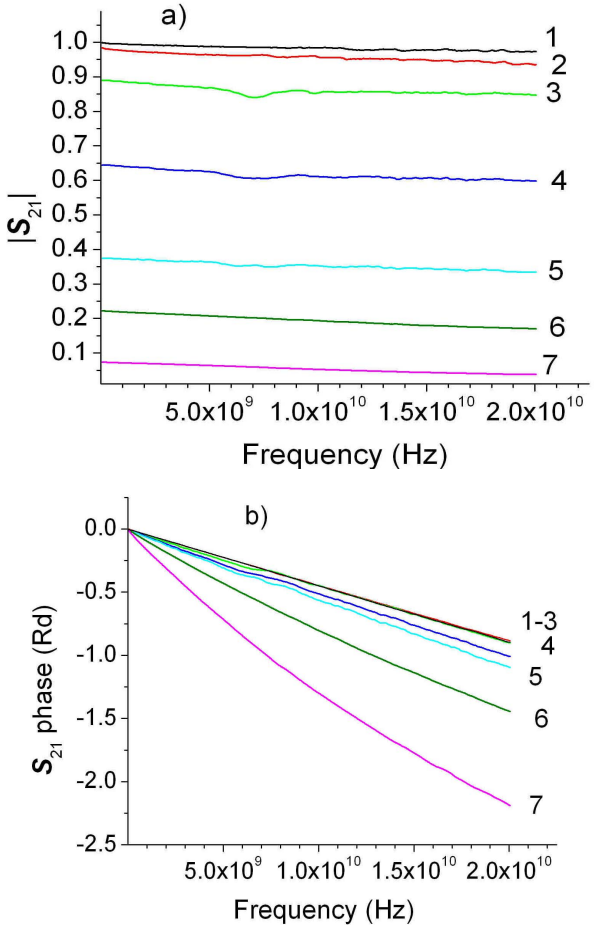

Figure 2. (a) - S_{21} magnitude and phase (b) for uncoated CPW (1) and CPWs coated with the following Au film thickness: (2) – 4 nm, (3)-7 nm , (4)-8 nm, (5)- 8.5 nm, (6)-9 nm and (7)- 10 nm. The CPW length is 900 μm

B. *Conductance Reflectance and Transmittance*

The σ_s results obtained for the CPW substrate (plot 1) and for the Au films (plots 2-7) are shown in Fig. 3 in the frequency range of 1 GHz to 20 GHz. The surface conductance of the CPW substrate is about 5×10^{-7} S ± 2×10^{-7}S. At 10 GHz, the conductance, σ_s, of weakly conducting 4 nm thick Au films is about 4×10^{-6} S. Thicker films show considerably higher σ_s values with flat frequency characteristics.

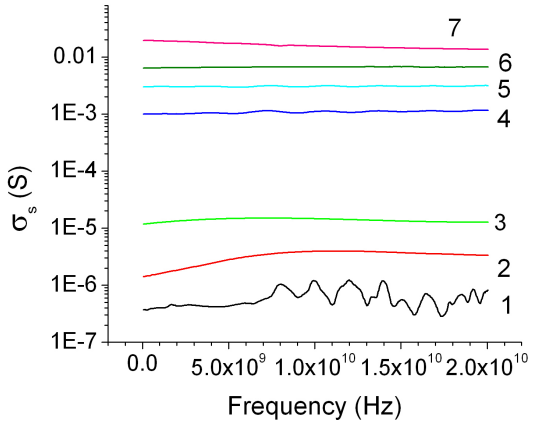

Figure 3. Surface conductance (σ_s) for uncoated CPW (1), and CPWs coated with the following Au film thickness:
(2) – 4 nm, (3)-7 nm, (4)-8 nm, (5)- 8.5 nm, (6)-9 nm, and (7)- 10 nm.
The uncertainty in plots 1 - 7 is 2×10^{-7}S.

At 10 GHz, σ_s of a 7 nm thick film is about 1.4×10^{-5} S, and this value increases further to about 1.5×10^{-2} S for films 10 nm thick. The corresponding bulk conductivity of 10 nm thick films is about 1.5×10^{4} S/cm, for which the skin depth is about 4.1 μm, more than two orders of magnitude larger than the film thickness. The frequency independent conductance in Fig. 3 is apparent and is probably the most interesting characteristic of granular metallic films with thickness smaller than the skin depth.

Figure 4 shows coefficients of the transmittance, $\tau = (e^{-\gamma l})(e^{-\gamma l})^*$ (Eq. 3a), reflectance, $\rho = \boldsymbol{\Gamma\Gamma}^*$, and dissipation, $\alpha = 1 - \rho - \tau$, plotted as a function of film thickness. It is seen

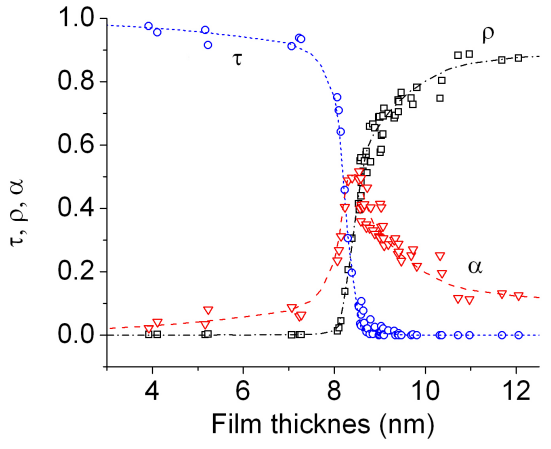

Figure 4. Transmittance (τ -circles), reflectance (ρ -squares) and dissipation (α - triangles), as a function of film thickness at 10 GHz. Dashed lines are plotted through the points as guides.

that the reflectance ρ of films thinner than 7 nm is near zero, while transmittance τ gradually decreases from 1.0 to about 0.9, which is balanced by an increase in loss. The films show a sharp transition from the insulating to the conducting state (percolation transition), at film thickness $d \approx 8$ nm. Within the percolation threshold, 8 nm < d < 9 nm, τ falls to zero, ρ increases steeply while the dissipation coefficient α (loss) reaches a peak value of about 0.5 (figure 4). In this narrow thickness range, the semicontinuous films show non-classical behavior. Aggregation of the metallic nanoparticles towards the percolation point, where positive dielectric and negative metallic permittivities merge, creates a singularity, which results in a large fluctuation of the local density of electronic states [10]. Above the percolation transition, films with $d > 10$ nm show properties of a continuous conductor. Reflectance approaches a constant value of 0.9, $\tau \approx 0$ and α decreases to about 0.1. Above the percolation transition transmittance is negligible and the microwave properties are described exclusively by reflectance and loss.

Earlier microwave reflectance-transmittance experiments conducted in free space on thin metallic films showed difficulty in quantifying loss due to the enormous impedance mismatch between air and metal at these centimeter wavelengths [11]. In the presented CPW configuration, the effective impedance matching is achieved readily, and the propagation characteristic can be defined and accurately normalized to the CPW propagation length.

IV. CONCLUSSION

We employ a coplanar waveguide configuration to measure surface conductance of thin semicontinuous films. The formulas that correlate the two port scattering parameters, $\mathbf{S}_{11}$ and $\mathbf{S}_{21}$, with the distributed circuit parameters of the specimen are given in closed form. The experimental results are illustrated on vapor deposited gold films, 4 nm to 12 nm thick. The characteristic crossover transition from the insulating to the conducting state occurs in the narrow thickness range, at film thickness $d \approx 8$ nm. Our measurements of both $\mathbf{S}_{11}$ and $\mathbf{S}_{21}$ capture this transition with a high accuracy that is unobtainable by the one-port $\mathbf{S}_{11}$ reflectometry or free space techniques. Above the percolation threshold, films thicker than 10 nm show a high conductivity typical for a continuous conductor. The frequency independent conductance and large dissipation in the vicinity of the percolation threshold are the interesting non-classical characteristic of semicontinuous films with thickness smaller than the skin depth.

[1] M. Walther, D. G. Cooke, C. Sherstan, M. Hajar, M. R. Freeman, and F. A. Hegmann, Phys. Rev. B **76**, 125408 (2007).

[2] V. Antonets, L. N. Kotov, S. V. Nekipelov and E. N. Karpushov, Technical Physics, **49**, 1496 (2004).

[3] JM. D. Janezic and D. F. Williams; IEEE MTT-S Int. Microwave Symp. Dig. **3**, 1343-6 (1977).

[4] V. Milanovic, M. Ozgur, D. C. DeGroot, J. A. Jargon, M. Gaitan, and M. E. Zaghloul; IEEE Trans. Microwave Theor. Tech. **46**, 632 (1998).

[5] J. Obrzut, *Springer Handbook of Metrology and Testing*, Eds., Czichos, H.; Saito, T.; Smith, L.; New York: Springer, 2011, pp. 532.

[6] S. Rao, J. R. Whinnery, T. Van Duzer, *Communication Electronics*, J. Wiley, New York, pp. 414 (1993).

[7] M. Nicolson, IEEE Trans. Instrum. Meas. **19**, 337–382 (1970).

[8] J. Baker-Jarvis, R. G. Geyer, P. D. Domich,. IEEE Trans. Instrum. Meas **41**, 646–652 (1992).

[9] W. R. Eisenstadt and Y. Eo, IEEE Trans. Components, Hybr. Manufact. Tech., **15** 483-490 (1992).

[10] V. Krachmalncoff, E. Castanie, Y. De Wlde, and R. Carminati, Phys. Rev. Lett., **105**, 183901 (2010).

[11] I. R. Hooper, J. R. Sambles, Optics Express **16**, 17249 (2008).